ELSEVIER

A hybrid finite element formulation for a beam-plate system

Sang Bum Hong, Aimin Wang, Nickolas Vlahopoulos*

*Department of Naval Architecture and Marine Engineering, The University of Michigan, 2600 Draper Road, Ann Arbor,
MI 48109-2145, USA*

Abstract

A new development in the area of the hybrid finite element analysis (hybrid FEA) is presented. The hybrid FEA method combines the conventional FEA method with energy FEA (EFEA) for analysis of systems that contain both flexible and stiff members. A formulation for analyzing flexible plates spot-welded to stiff beams when the excitation is applied on the stiff members is developed. Conventional FEA models are employed for modeling the behavior of the stiff members in a system. Appropriate damping elements are introduced in the connections between stiff and flexible members in order to capture the presence of the flexible members during the analyses of the stiff ones. The component mode synthesis method is combined with analytical solutions for determining the driving point conductance at joints between stiff and flexible members and for defining the properties of the damping elements which represent the flexible members when analyzing the stiff components. Once the vibration of the stiff members and the amount of power dissipated at the damping elements has been identified, an EFEA analysis is performed in order to determine the amount of vibrational energy in the flexible members. The new developments are validated by comparing results of the hybrid FEA with results from very dense conventional finite element analyses for structures of increasing complexity.
© 2006 Elsevier Ltd. All rights reserved.

1. Introduction

The frequency spectrum for vibration analyses can be divided into three regions—low, mid, and high—according to the number of wavelengths present in all the important components of the system which is analyzed. The low-frequency region is defined as the range in which all components contain a small number of wavelengths and behave as stiff members. Stiff members exhibit resonant behavior and have low modal overlap values. The modal overlap values are defined as the resonance bandwidth divided by the average frequency spacing between resonance frequencies. The characteristic of low modal overlap enables us to consider each mode of the stiff members separately. Conventional FEA is a practical numerical approach for simulating low-frequency vibrations using either modal or a direct frequency response method [1–3].

At the opposite end of the spectrum, the high-frequency region is defined as the range in which all the important components in the system which is analyzed contain a large number of wavelengths and they behave as flexible members. Flexible members exhibit considerably higher modal overlap than the stiff

---

*Corresponding author. Tel.: + 1 734 764 8341; fax: + 1 734 936 8820.

E-mail address: nickvl@engin.umich.edu (N. Vlahopoulos).

members, since multiple resonances are present. For simulating high-frequency vibrations, statistical energy analysis (SEA) [4–8] and EFEA [9–17] can be used. Both methods provide meaningful results for the ensemble average response of each member and of the system [18].

The mid-frequency region is defined as the range in which some of the components of a system behave as stiff members, while other components possess characteristics of flexible members. In the mid-frequency range, neither the FEA nor the energy-based methods (SEA and EFEA) are suitable for an efficient and valid analysis. Specifically, FEA method requires a prohibitively large number of computations in order to capture the vibration of the flexible members. In addition FEA methods provide results at discrete locations and frequencies. In order to generate meaningful information for the flexible members of a system in mid-frequency ranges space averaged and frequency averaged results must be generated. This requires large amounts of disk storage for saving the data generated from conventional FEA computations. Recently, efforts have been presented for performing conventional FEA analyses with greater efficiency in order to extend the frequency range where a conventional FEA analysis is practical [19–21]. The energy-based methods contain assumptions that are valid when all components of a system are flexible and exhibit behavior that can be approximated as incoherent. Thus, when the stiff members are important in the power transfer mechanism the energy methods cannot capture the resonant effects that are present due to the stiff members of a system in the mid-frequencies.

In the past several approaches have been pursued for enabling computations for systems with a large number of components and for performing analyses in mid-frequency ranges. The fuzzy structure theory was introduced in order to predict the response of a master structure coupled with a large number of secondary structures attached to the master structure [22–26]. The attached subsystems are called fuzzy substructures and are considered as difficult to model using conventional methods due to their complexity in geometry or physical properties. The primary objective of the fuzzy structure theory is to compute the response of the master structure while accounting for the influence of all the secondary structures. The effects of the fuzzy substructures on the master structure below the first eigenfrequency of the fuzzy substructure are mainly due to added-mass effects. Above the first eigenfrequency of the fuzzy substructures, the presence of the fuzzy substructures induces damping to the master structure. The effect of this damping transfers a certain amount of mechanical energy from the master structure to the fuzzy structure. A random boundary impedance operator was introduced in order to describe the effects of mass and damping of fuzzy substructures on the master structure in the mid-frequency range. The random boundary impedance operator was constructed using the concept of a type I or type II homogeneous fuzzy impedance law which depended on a set of parameters called the mean coefficients and the deviation coefficients of the law. The type I, which is a special case of the type II, can be used for a locally homogeneous boundary condition without an effect of a spatial memory into the fuzzy subsystems. By introducing additional mean and deviation coefficients, the type II can consider a spatial memory effect inside the fuzzy substructures. The Ritz–Galerkin method was utilized for a master structure coupled with fuzzy substructures using the structural modes of the master structure uncoupled with the fuzzy substructures. A finite element discretization of the master structure coupled with the fuzzy substructures was employed for accomplishing a numerical solution. Homogeneous cantilever beams with fuzzy subsystems of types I and II were studied [22], and the solutions were compared with Monte Carlo simulation results. The acoustic field radiated by a structure immersed in water was computed [22]. The primary structure was a slender steel shell cylinder having a large number of transverse stiffeners, a few transverse walls, and several internal three-dimensional subsystems. The type I fuzzy substructure was applied on all the inner side of the shell. Two rectangular simply supported plates with four substructures were analyzed [27]. The master structure was computed by the two plates connected along their common edge. The fuzzy subsystems were constituted of a rectangular homogeneous thin plate on which simple linear oscillators were attached.

An approach for determining the energy flow from a deterministic FEA was presented in Ref. [28]. The FEA was employed for determining the subsystem mass and stiffness matrices. The component mode synthesis (CMS) approach was used for performing the finite element analysis for each subsystem for computational efficiency. Three plates connected together at a corner configuration were analyzed.

A hybrid method for the analysis of complex structures comprised from stiff beams and flexible plates was presented in Refs. [29,30]. The approach in Refs. [29,30] separates the stiff parts of the structure from the

flexible parts and models each set of parts separately in order to accommodate the significantly different wavelengths of waves. Then it combines the two parts in order to obtain the response of the complete structural system. The plates were modeled as receiver impedances when analyzing the stiff beam members using the finite element method. The same rationale is employed in the work presented in this paper.

In the past, a hybrid approach was suggested for combining FEA and SEA formulations for mid-frequency computations [31]. In order to connect the variables of the FEA and SEA, an optimization routine was developed; this routine approximates the compatibility at the joint between the SEA and the FEA variables [31]. A hybrid SEA method based on partitioning the response of the system into global and local components was presented [32]. The distinction between the two types of components is based on their corresponding wavelengths of the response. The global component was intended to capture long wavelength deformations, whereas the local component was related to short wavelength deformations. The solution method consisted of a deterministic model of the global response and an SEA model of the local response. The global equations of motion included a contribution to the dynamic stiffness matrix and the forcing vector arising from the presence of the local response. The main effect of the local mode dynamics was to add damping and effective mass to the global modes, similar to the fuzzy structure theory. The local mode response was computed using SEA. This equation included an input power term which originated from the presence of the global modes. This hybrid method was applied to systems composed of rod elements [32].

A hybrid FEA formulation has been developed for mid-frequency analysis of collinear or planar beam systems [33–36]. The hybrid FEA approach combines conventional FEA with EFEA to achieve a numerical solution for systems comprised by stiff and flexible members. Stiff and flexible members are modeled by conventional FEA and EFEA, respectively. The EFEA is selected to be coupled with the low-frequency methods because it is based on a spatial discretization of the system that is being modeled. Thus, it is possible to develop appropriate interface conditions at the joints between the primary variables of the EFEA models of the flexible members and the FEA models of the stiff members. The hybrid FEA utilized for systems of collinear beams with excitations applied either on flexible members [33], or on stiff members [34], for studying the power flow characteristics for systems of collinear beams [35], and for modeling the vibration of beams connected at an arbitrary angle [36].

In this paper, the hybrid FEA is extended to more complex systems comprised of flexible plates spot-welded to a stiff frame structure made of tubular beams. The concepts introduced by the fuzzy structure theory [22–27] of representing attached components as damping elements, and by the hybrid analytical FEA approach [29,30] of separating a structure in flexible and stiff parts and modeling the flexible parts as receiver impedances when analyzing the stiff members, are combined with the FEA and EFEA methods in this paper. Appropriate damping elements are introduced in the FEA model of the stiff members in order to capture the effect of the flexible members. The values of the damping elements in this work are evaluated from the driving point impedance of the flexible members. The latter is computed by applying a CMS approach with the analytical solution for the vibration of a rectangular plate. Once the vibration of the stiff members is evaluated the power input into the flexible members is determined and an EFEA analysis is performed for determining the amount of energy in the flexible members. The new hybrid FEA formulation is validated through comparison with very dense conventional FEA models for several structural systems of increasing complexity.

2. Background on the component mode synthesis method

Since the CMS method is used in this paper for approximating the power flow from a stiff to a flexible member, a brief overview of the method is presented. In the CMS method, a structure is considered to be composed of interior and boundary degrees of freedom (dof) [37,38]. The displacement of the internal dof is considered as a linear superposition of the internal normal modes (computed with all the boundary dof fixed) and the constraint modes. Constraint modes are the static displacements introduced in the internal dof due to a unit displacement imposed on a single boundary dof while all other boundary dof are fixed. The boundary dof are expressed in terms of their actual physical values.

For an undamped system the equations of motions for the CMS method are:

$$\begin{bmatrix} I & 0 \\ \phi^C & \phi^N \end{bmatrix}^T [m] \begin{bmatrix} I & 0 \\ \phi^C & \phi^N \end{bmatrix} \begin{Bmatrix} \ddot{\delta}^B \\ \ddot{p}^N \end{Bmatrix}$$
$$+ \begin{bmatrix} I & 0 \\ \phi^C & \phi^N \end{bmatrix}^T [k] \begin{bmatrix} I & 0 \\ \phi^C & \phi^N \end{bmatrix} \begin{Bmatrix} \delta^B \\ p^N \end{Bmatrix} = \begin{bmatrix} I & 0 \\ \phi^C & \phi^N \end{bmatrix}^T \begin{Bmatrix} F^B \\ F^I \end{Bmatrix}, \tag{1}$$

where $[m] =$ mass matrix, $[k] =$ stiffness matrix, $\{\delta^B\} =$ physical displacements at the boundary dof, $\{F^B\} =$ vector of external force at the boundary dof, and $\{F^I\} =$ vector of external force at the internal dof. Superscripts B and I refer to boundary and interior dof, respectively. $[\phi^C] =$ modal matrix containing the constraint modes, $[\phi^N] =$ modal matrix of the internal normal modes, and $\{p^N\} =$ vector of the modal coordinates of the internal normal modes. Eq. (1) can be expressed in the modal coordinate system as

$$\begin{bmatrix} m^{BB} & m^{BI} \\ m^{IB} & m^{II} \end{bmatrix} \begin{Bmatrix} \ddot{\delta}^B \\ \ddot{p}^N \end{Bmatrix} + \begin{bmatrix} k^{BB} & k^{BI} \\ k^{IB} & k^{II} \end{bmatrix} \begin{Bmatrix} \delta^B \\ p^N \end{Bmatrix} = \begin{Bmatrix} \bar{F}^B \\ \bar{F}^I \end{Bmatrix}, \tag{2}$$

where $\{\bar{F}^B\} =$ modal forces applied on the boundary dof, and $\{\bar{F}^I\} =$ modal forces applied on the internal dof. According to [38], the matrices k^{BI} and k^{IB} are null due to the way in which the coordinate transformation matrix

$$\begin{bmatrix} I & 0 \\ \phi^C & \phi^N \end{bmatrix}$$

has been defined in Eq. (1). Finally, the equation of motion in the modal coordinate system becomes

$$\begin{bmatrix} m^{BB} & m^{BI} \\ m^{IB} & m^{II} \end{bmatrix} \begin{Bmatrix} \ddot{\delta}^B \\ \ddot{p}^N \end{Bmatrix} + \begin{bmatrix} k^{BB} & 0 \\ 0 & k^{II} \end{bmatrix} \begin{Bmatrix} \delta^B \\ p^N \end{Bmatrix} = \begin{Bmatrix} \bar{F}^B \\ \bar{F}^I \end{Bmatrix}. \tag{3}$$

3. Hybrid FEA formulation

The bending behavior of the plates (flexible members) is modeled by the EFEA formulation and the in-plane behavior of the plates and the overall behavior of the tubular beam members (stiff members) are modeled with conventional FEA. The effect of the flexible members on the behavior of the stiff members is modeled by adding damping elements in the FEA model of the stiff members. The appropriate values of the damping elements are computed from the conductance at the spot-welded connections between the flexible and the stiff members. In high-frequency methods (SEA, EFEA) a typical approach for evaluating the conductance is through the analytical expression for the driving point impedance of an infinite or a semi-infinite plate. An alternative approach is presented in this paper which takes into account the modal and the damping characteristics of the plate. A CMS approach is applied on an analytical solution for deriving the conductance. The external excitation is considered to be applied only on the stiff members. The vibration of the stiff members and the amount of power flow to the flexible members through the spot-welded connections are obtained first. The latter comprises the excitation for the EFEA analysis which determines the amount of bending energy in the plate members. The computational procedure of the hybrid FEA is outlined in Fig. 1.

3.1. Evaluation of conductance at the spot-welded connections between stiff and flexible members

For the derivation of the conductance each flexible plate member is idealized as a rectangular plate similar to the SEA approach when evaluating modal characteristics for a subsystem of bending modes of a plate. According to the CMS method the bending dof of the rectangular plate are partitioned into the boundary and the interior dof. Therefore, the displacement of any point P of the plate is considered as a superposition of two
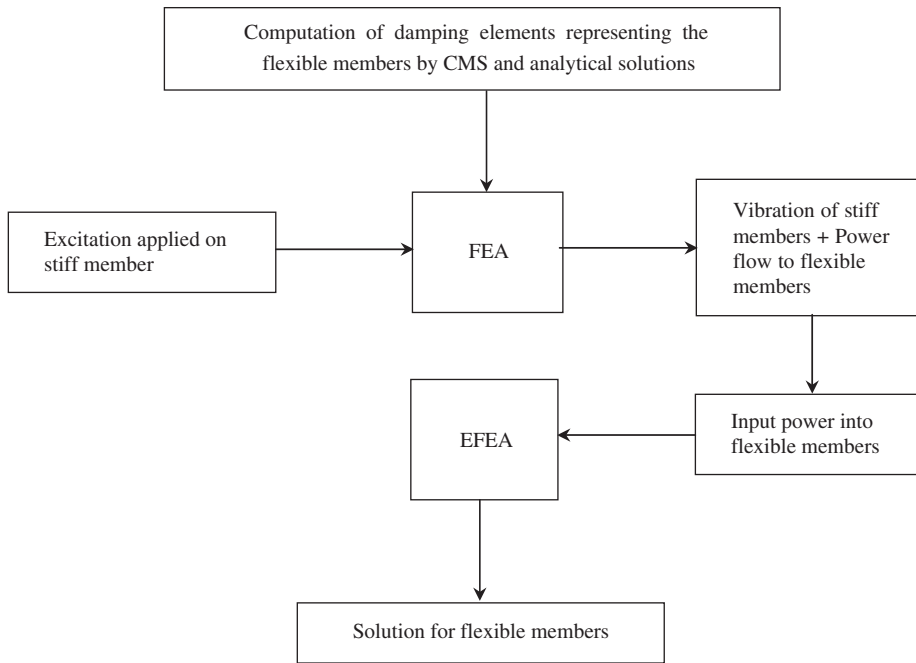
Fig. 1. Flow chart of the hybrid FEA computational process.

components, one induced by the movement of the boundary dof and the other from the relative motion of the interior dof with respect to the boundary dof. The constraint modes are employed for defining the former and the internal normal modes are employed for determining the latter. The structural damping of the plate is considered in the derivation through the modulus of elasticity for the plate. The displacement at point P can be written as

$$w(x, y, t) = w^{(i)}(x, y, t) + w^{(c)}(x, y, t), \tag{4}$$

where $w^{(i)}(x, y, t)$ is the relative motion of the interior dof with respect to the boundary. $w^{(i)}(x, y, t)$ is represented as a linear superposition of the internal mass-normalized normal modes $\psi_{mn}(x, y)$, while $Y_{mn}(t)$ are the corresponding modal coordinates:

$$w^{(i)}(x, y, t) = \sum_{m,n} Y_{mn}(t)\psi_{mn}(x, y) \tag{5}$$

$w^{(c)}(x, y, t)$ is the displacement induced by the movement of the boundary dof at the location where the conductance is evaluated:

$$w^{(c)}(x, y, t) = Y_s(t)\psi_s(x, y), \tag{6}$$

where $\psi_s(x, y)$ is the constraint mode derived by considering a unit displacement at the spot-welded boundary dof where the conductance is computed while all the remaining spot-welded boundary dof are fixed, and $Y_s(t)$ is the corresponding generalized coordinate. Since the conductance is evaluated for only one spot-welded boundary dof at a time, only one constraint mode is considered in the computations.

Combining Eqs. (4)–(6) results in

$$w(x, y, t) = \sum_{m,n} Y_{mn}(t)\psi_{mn}(x, y) + Y_s(t)\psi_s(x, y). \tag{7}$$

Eq. (7) provides the displacement throughout the plate in terms of the CMS dof.

Introducing the displacement expression from Eq. (7) into the governing differential equation for the bending vibration of a plate results in

$$D\left(\sum_{m,n} Y_{mn}(t)\nabla^4\psi_{mn}(x,y) + Y_s(t)\nabla^4\psi_s(x,y)\right)$$
$$+ \rho_s\left(\sum_{m,n} \ddot{Y}_{mn}(t)\psi_{mn}(x,y) + \ddot{Y}_s(t)\psi_s(x,y)\right) = f(x,y,t), \tag{8}$$

where $D = Et^3/12(1-v^2)$ = the flexural rigidity, ρ_s = the mass density per area, $f(x,y,t)$ = the external force, and $\nabla^4 = \nabla^2\nabla^2$, where ∇^2 is the Laplacian operator.

Since the displacements on the perimeter of a simply supported plate comprise the boundary dof, then the internal normal modes and the corresponding fourth-order derivatives are expressed in terms of the mode shapes of a simply supported rectangular plate [5]. The static mode is expressed in a polynomial form:

$$\psi_s = (1 + a_1 x + a_2 x^2 + a_3 x^3 + a_4 x^4) \times (1 + b_1 y + b_2 y^2 + b_3 y^3 + b_4 y^4 + b_5 y^5). \tag{9}$$

In order to obtain the coefficients of a's and b's in Eq. (9), a static analysis is conducted for the plate using conventional FEA. All the nodes at the spot-welded connections on the perimeter of the plate are constrained except the node where the conductance is computed. A small number of finite elements are required for performing the static finite element analysis. A two dimensional polynomial regression is performed for obtaining the coefficients in Eq. (9). Introducing the analytical expressions for the internal and the constraint normal modes and considering harmonic time dependency in Eq. (8) results in

$$D\sum_{m,n}\left[\left(\frac{m\pi}{L_x}\right)^2 + \left(\frac{n\pi}{L_y}\right)^2\right]^2 Y_{mn}\psi_{mn} - \rho_s\omega^2\sum_{m,n} Y_{mn}\psi_{mn} + DY_s\nabla^4\psi_s - \rho_s\omega^2 Y_s\psi_s = f, \tag{10}$$

where L_x and L_y are the lengths of the rectangular plate in x and y directions, respectively. Multiplying Eq. (10) with an internal normal mode, ψ_{kl}, and integrating over the domain A, results in

$$-\omega^2\left(Y_s\int_A \psi_{kl}\psi_s\,\mathrm{d}A + \sum_{m,n} Y_{mn}\int_A \psi_{mn}\psi_{kl}\,\mathrm{d}A\right)$$
$$+ \frac{D}{\rho_s}Y_s\int_A \psi_{kl}\nabla^4\psi_s\,\mathrm{d}A + \sum_{m,n}\omega_{mn}^2 Y_{mn}\int_A \psi_{mn}\psi_{kl}\,\mathrm{d}A = \frac{1}{\rho_s}\int_A f\psi_{kl}\,\mathrm{d}A. \tag{11}$$

The four terms on the left-hand side of Eq. (11) correspond to m^{IB}, m^{II}, k^{IB}, and k^{II} of Eq. (2), respectively. The second and fourth terms of Eq. (11) are nonzero only when $m = k$ and $n = l$ because of the orthogonality of the internal normal modes. The third term in Eq. (11) is set equal to zero according to the CMS method [37]. Since the objective of this derivation is to evaluate the conductance at a single spot-welded point on the outer boundary of the plate, the external force $f(x,y,t)$ is considered to be applied on one of the boundary dof. Thus, the right hand side of Eq. (11) is equal to zero since the external force is always applied on a boundary dof where the displacement of any internal normal mode, ψ_{kl}, is always equal to zero. Solving Eq. (11) for the modal coordinates of the internal normal modes results in

$$Y_{kl} = \frac{4\omega^2\int_A \psi_s\psi_{kl}\,\mathrm{d}A}{L_x L_y(\omega_{kl}^2 - \omega^2)}Y_s. \tag{12}$$

Eq. (12) provides the relationships between the generalized coordinate of the constraint mode and the modal coordinates of all the internal normal modes. The coupling between the internal and the constraint modes originates from the inertia term in the numerator. Multiplying Eq. (10) with the constraint mode, ψ_s, and

integrating over the entire domain A, results in

$$-\omega^2\left(Y_s\int_A\psi_s\psi_s\,\mathrm{d}A + \sum_{m,n}Y_{mn}\int_A\psi_{mn}\psi_s\,\mathrm{d}A\right) + \frac{D}{\rho_s}Y_s\int_A\psi_s\nabla^4\psi_s\,\mathrm{d}A$$
$$+\sum_{m,n}\omega_{mn}^2Y_{mn}\int_A\psi_{mn}\psi_s\,\mathrm{d}A = \frac{1}{\rho_s}\int_A f\psi_s\,\mathrm{d}A. \tag{13}$$

The four terms on the left-hand side of Eq. (13) correspond to m^{BB}, m^{BI}, k^{BB}, and k^{BI} of Eq. (2), respectively. The fourth term of Eq. (13) is set equal to zero according to the CMS approach [37]. The term on the right-hand side represents the work done by the external force which is applied on the boundary dof where the conductance is computed. Utilizing the relationship between the modal coordinates of the internal normal modes and the generalized coordinate of the constraint mode results in

$$-\frac{4\omega^4}{L_xL_y}\sum_{m,n}Y_s\left(\frac{\int_A\psi_s\psi_{mn}\,\mathrm{d}A}{(\omega_{mn}^2-\omega^2)}\right)\int_A\psi_{mn}\psi_s\,\mathrm{d}A$$
$$+\frac{D}{\rho_s}Y_s\int_A\psi_s\nabla^4\psi_s\,\mathrm{d}A - \omega^2Y_s\int_A\psi_s\psi_s\,\mathrm{d}A = \frac{1}{\rho_s}\int_A f\psi_s\,\mathrm{d}A. \tag{14}$$

As observed in Ref. [32] one of the choices of basis functions for representing the displacement function $w(x,y,t)$ are the blocked modes and the constraint modes. This selection of basis functions is employed in this paper. The underlying approach which is utilized here originates from the basis of fuzzy structure theory [23]. It is more relevant to [29,30] where a structure was separated in flexible and stiff parts, and the flexible parts were modeled as receiver impedances when analyzing the stiff members. The generalized coordinate of the constraint mode is finally obtained from Eq. (14) as

$$Y_s = \left[-\frac{4\rho_s\omega^4}{L_xL_y}\sum_{m,n}\left(\frac{\int_A\psi_s\psi_{mn}\,\mathrm{d}A}{\omega_{mn}^2-\omega^2}\right)\int_A\psi_{mn}\psi_s\,\mathrm{d}A + D\int_A\psi_s\nabla^4\psi_s\,\mathrm{d}A - \rho_s\omega^2\int_A\psi_s\psi_s\,\mathrm{d}A\right]^{-1}\int_A f\psi_s\,\mathrm{d}A. \tag{15}$$

Since all boundary dof for the internal normal modes are fixed, the displacement at the perimeter of the plate is expressed only in terms of the constraint mode. Considering a unit external force applied at the location (x_0,y_0) where the conductance is computed, an expression is derived for the value of the admittance, $M(x_0,y_0)$, at the point where the excitation is applied:

$$M(x_0,y_0,t) = j\omega Y_s(x_0,y_0,t)\psi_s(x_0,y_0). \tag{16}$$

The conductance is the real part of the admittance, and corresponds to the inverse of the damping coefficient which identifies the amount of power absorbed from the external excitation due to the vibration of the plate:

$$G(x_0,y_0,t) = \mathrm{Re}\big[M(x_0,y_0,t)\big] = \mathrm{Re}\big[j\omega Y_s(x_0,y_0,t)\psi_s(x_0,y_0)\big]. \tag{17}$$

Since the static mode, ψ_s, is defined so that the magnitude of the static mode at the location (x_0,y_0) where the conductance is computed is equal to one unit, and considering that the external force has a unit amplitude, the corresponding conductance value is

$$G(x_0,y_0,t) = \mathrm{Re}\big[M(x_0,y_0,t)\big] = \mathrm{Re}\big[j\omega Y_s(x_0,y_0,t)\big]. \tag{18}$$

The conductance is employed in the FEA model of the stiff members to represent the effect of the flexible members on the vibration of the stiff members and for determining the amount of power absorbed by the flexible members.

3.2. Time averaged input power to flexible members

At every point where a flexible member is connected to a stiff member appropriate concentrated damping elements are attached to the FEA model in order to model the apparent damping induced by the power flow between the flexible member and the stiff member. The values of the concentrated damping elements are determined from Eq. (18). Since the external excitation is considered to be applied on the stiff members the

vibration of the stiff members is computed first. Based on the vibration of the stiff members at the spot-welded attachment points and the values of the damping elements, the power flow to the flexible members is determined for each attachment point:

$$Q_{\mathrm{in}} = \langle F \cdot v \rangle = \langle v^2 \rangle / G(x_0, y_0, t), \tag{19}$$

where F represents the force exerted on the flexible member from the stiff member at the spot-welded attachment point (x_0, y_0), v is the corresponding transverse velocity of the flexible member at the attachment point (x_0, y_0) which is equal to the transverse velocity of the stiff member at the attachment point (x_0, y_0) based on the displacement compatibility at that point, and $\langle \ \rangle$ represents the time average of the quantity inside the bracket. The power flow at each spot-welded attachment point (x_0, y_0) defines the excitation at the corresponding locations of the EFEA model of the flexible members.

4. Validation and application

Several structures of increasing complexity are analyzed using the new hybrid FEA formulation and the results are always compared to solutions computed by very dense conventional FEA models. The general purpose FEA code NASTRAN is utilized for performing the analysis for the stiff members in the hybrid FEA solution, and for all the conventional FEA computations. By setting the proper parameters in PSHELL entry, NASTRAN can automatically decouple the bending (out-of-plane) behavior from the in-plane behavior for either flat plate structures or the shells with curvatures [39]. In all the applications where a dense FEA model was utilized the size of the elements was determined in a manner that six linear elements were present within each wavelength of vibration at the highest frequency of analysis. The structural damping in all the applications is 2%.

4.1. Computation of the conductance for a rectangular plate

Typical results for the value of the conductance evaluated by the new hybrid FEA approach are presented first. Computations are performed for a rectangular plate which is 1.63 m wide, 1.09 m long, has structural damping of 2% and thickness of 0.8 mm. The plate is connected to the frame through 78 uniformly distributed spot-welded points along the perimeter of the plate. To calculate the conductance, the displacements are constrained at all the spot-welded attachment nodes at the perimeter of the plate except a single attachment
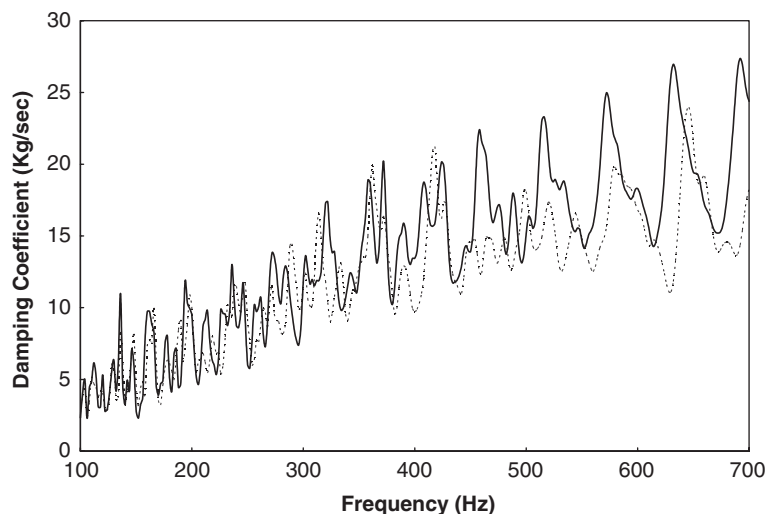

Fig. 2. Comparison of conductance (damping coefficient) curve of the plate (1.63 m × 1.09 m × 0.8 mm), - - - - analytical solution, ——— conventional FEA.

node where the conductance is computed. The node is located close to the center of the long side of the plate. The damping coefficient for each frequency of analysis is computed from the analytical Eq. (18) and from the driving point admittance of a very dense FEA model. Results from both computations are presented in Fig. 2 and good agreement is observed. The dense FEA results tend to diverge from the new analytical hybrid formulation only at the high end of the frequency range which is analyzed. This is a frequency range where the conventional FEA results become less reliable, therefore the correlation between the two solutions is considered acceptable.

4.2. Validation and applications of hybrid FEA

Typical results from analyses of structures with increasing complexity are presented. In the validations the results of a very dense FEA model are compared to the hybrid FEA results. The agreement between three sets of results is evaluated. First, the amount of input power into the system is compared between the two methods. Since the external excitation is defined as a force applied on the structure it is important for the corresponding input power to be comparable. Convergence indicates that the power dissipation mechanism and the driving point conductance of the entire structure are computed correctly by the hybrid formulation. The structural vibration at selected points of the stiff members comprises another measurable. Agreement between the two
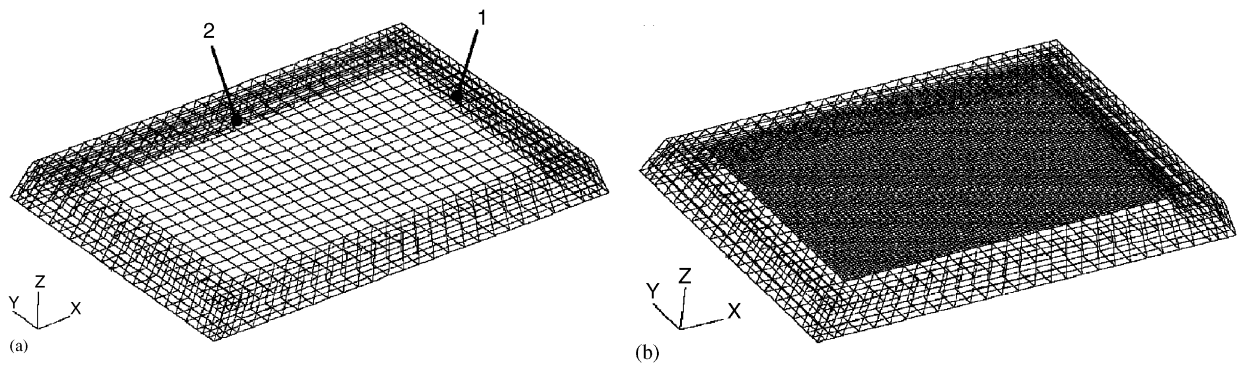
Fig. 3. Simple case with a plate and beams (a) for hybrid FEA, 6915 dof, (b) for FEA, 52,533 dof.
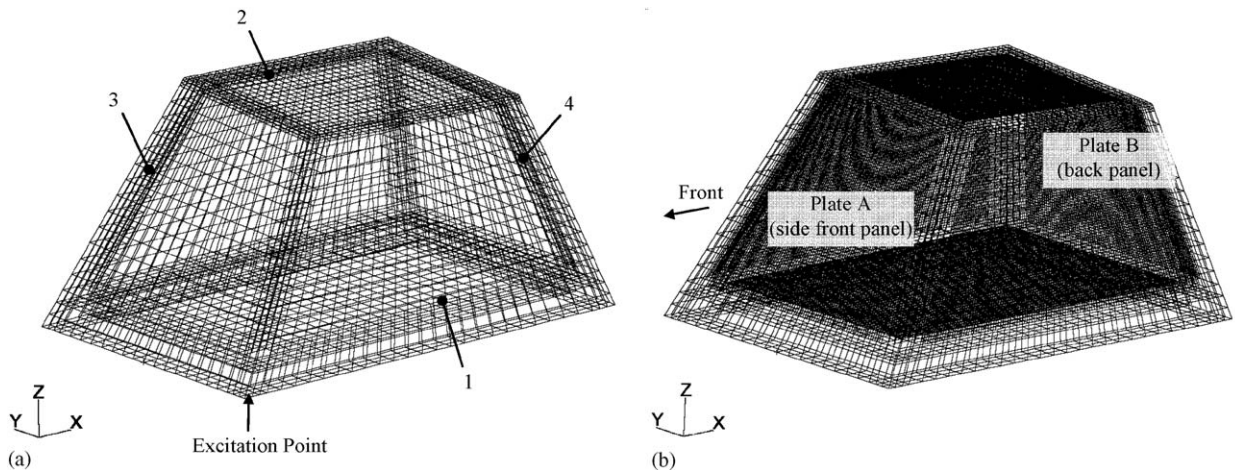
Fig. 4. Box structure comprised by multiple plates and beams for (a) hybrid FEA: 18,034 dof, (b) FEA: 218,419 dof.
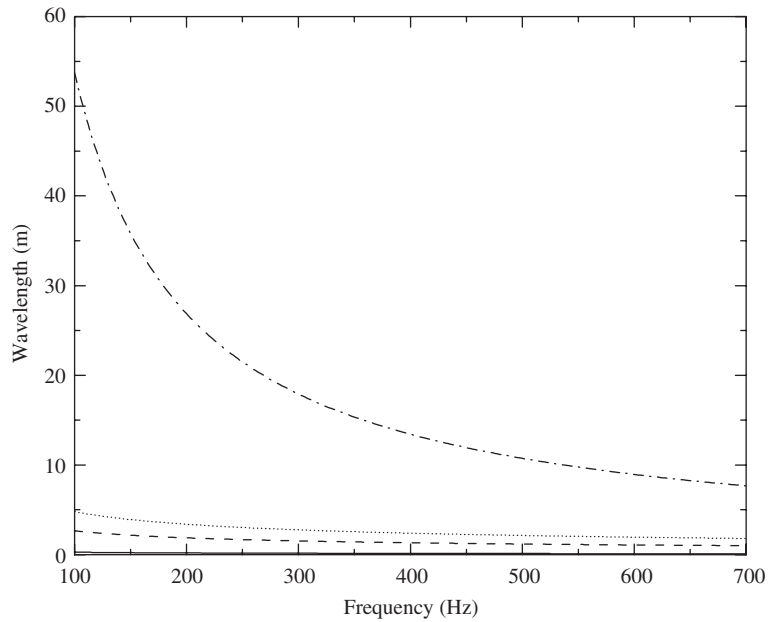
Fig. 5. Wavelengths of members of the box structure depicted in Fig. 4: from the bottom, bending property of plate ($t = 0.8$ mm), lower frame ($I = 5.7447e-6$ m^4, area $= 1.1291e-3$ m^2), upper frame ($I = 2.243e-7$ m^4, area $= 4.65e-4$ m^2), and in-plane property of plate ($t = 0.8$ mm). ——— Bending property of plate, - - - - upper frame, · · · · · lower frame, – – – in-plane property of plate.
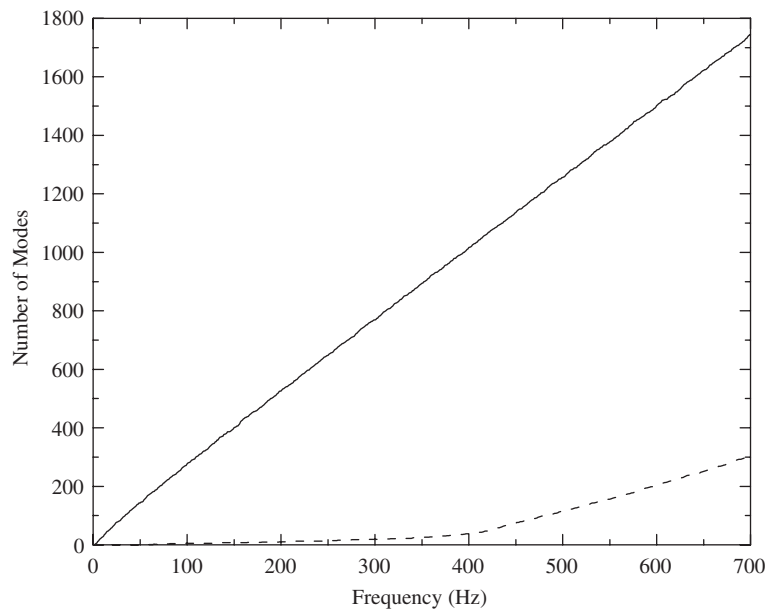

Fig. 6. Comparison of number of normal modes in flexible and stiff members for the box structure depicted in Fig. 4. ——— Flexible members (bending of plates), - - - - stiff members (in-plane motion plates and flexible behavior of beams).

solutions demonstrates that the effect of the flexible members is captured correctly in the hybrid FEA formulation. Finally, the amount of the energy in the flexible members is compared between the two methods in order to ensure that power flow into the flexible members is captured correctly and that the energy of the

flexible members is computed properly. Two structures with simple geometry are analyzed first and then computations are performed for an automotive BIW. A rectangular plate spot-welded connected to a frame made out of tubular beams (Fig. 3) is analyzed first, then computations are performed for a box structure made of multiple plates and tubular beams through spot-welded connection (Fig. 4). Finally, an automotive vehicle structure (Fig. 14) is analyzed. In order to demonstrate the relative rigidity of the stiff and the flexible members in the box structure, the wavelengths of the stiff and of the flexible members are presented in Fig. 5. It can be observed that the bending behavior of the plates flexible behavior due to the small dimension of the wavelengths, while the beam members, and the inplane behavior of the plates demonstrate stiff behavior by exhibiting considerably longer wavelengths in the frequency range of analysis. The values of the wavelengths presented in Fig. 5 are computed from analytical solutions of infinite plates and beams [40]. The number of normal modes of the stiff and the flexible members of the box structure computed by NASTRAN are also presented in Fig. 6. The number of normal modes of the flexible members is substantially higher than the number of normal modes in the stiff members in the mid-frequency range, and the increased demands on computational resources in the conventional FEA analyses originate from the behavior of the flexible members.
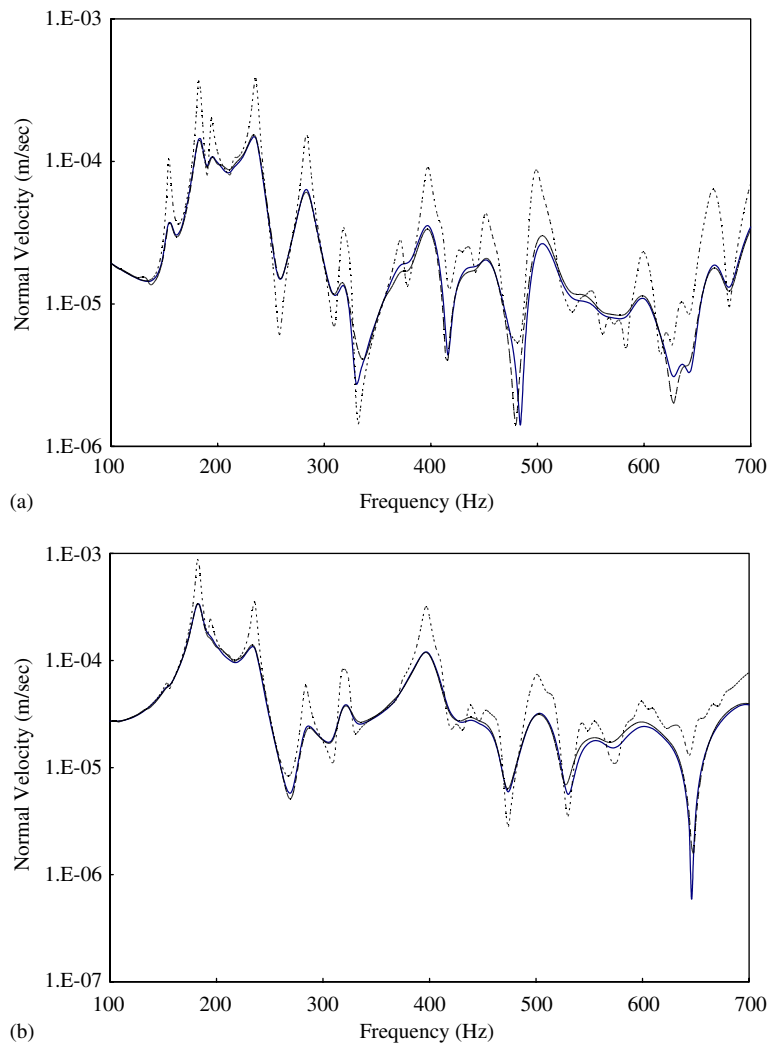
Fig. 7. Velocity at nodes 1 (a) and 2 (b) on the stiff members of the simple model depicted in Fig. 3. ——— Hybrid FEA, - - - - conventional FEA, · · · · · hybrid FEA without damper.

4.2.1. Results for the plate structure spot-welded connected to the tubular frame

The vibration velocities computed by the dense FEA and the hybrid method at two points of the frame structure marked on Fig. 3 are compared in Figs. 7(a) and (b). The velocities computed by the two different methods demonstrate very good correlation. This is an indication that the influence of the flexible member is captured properly during the FEA analyses of the stiff members. In order to demonstrate the importance of representing properly the flexible members when computing the behavior of the stiff members the damping elements which represents the presence of the flexible members are removed from the FEA model of the stiff members, and the vibration simulation are repeated. The velocities are overestimated in the peaks and underestimated in the valleys when the damping elements are removed. The difference in the results can be explained by the mechanism of energy dissipation. If the power dissipation from the flexible members is not accounted properly in the model, then the response of the stiff members is not computed correctly. Thus, it is important to account properly for the effect of the flexible members on the structural vibration of the stiff members. The results for the bending energy of the flexible plate computed by the hybrid FEA and the conventional dense FEA are presented in Fig. 8. Good correlation is observed between the results computed by the two methods. This is an indication that the power flow from the external excitation through the stiff members to the flexible members is captured correctly by the hybrid formulation.

4.2.2. Results for the box structure

A box with main dimension of 1.2 m wide, 2 m long, and 1 m height is analyzed (Fig. 4). It is comprised by plate members spot-welded connected to a frame made of tubular beam members. The properties of the tubular beam members are presented in Table 1 and the thickness of all the plates is 0.8 mm. An excitation
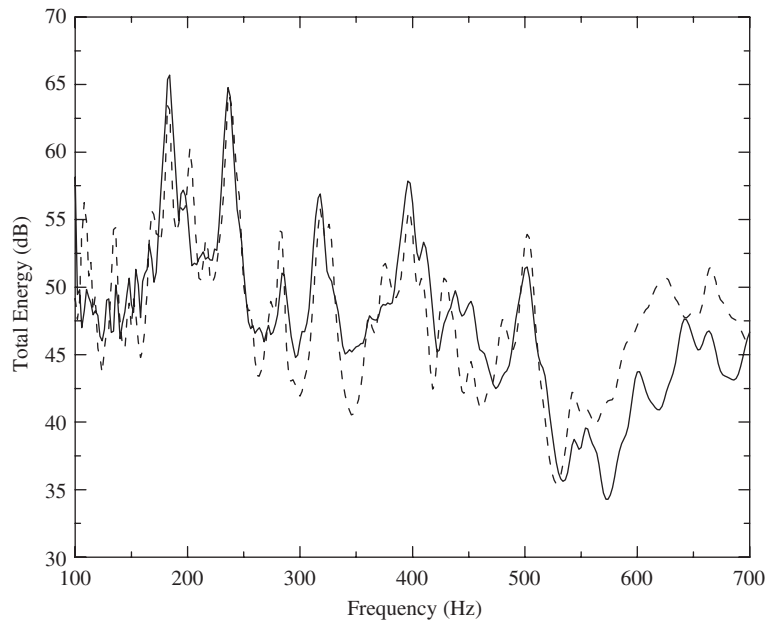
Fig. 8. Bending energy for the plate member of the simple model depicted in Fig. 3. ——— Hybrid FEA, - - - - conventional FEA.

Table 1
Properties of beams in the complex model

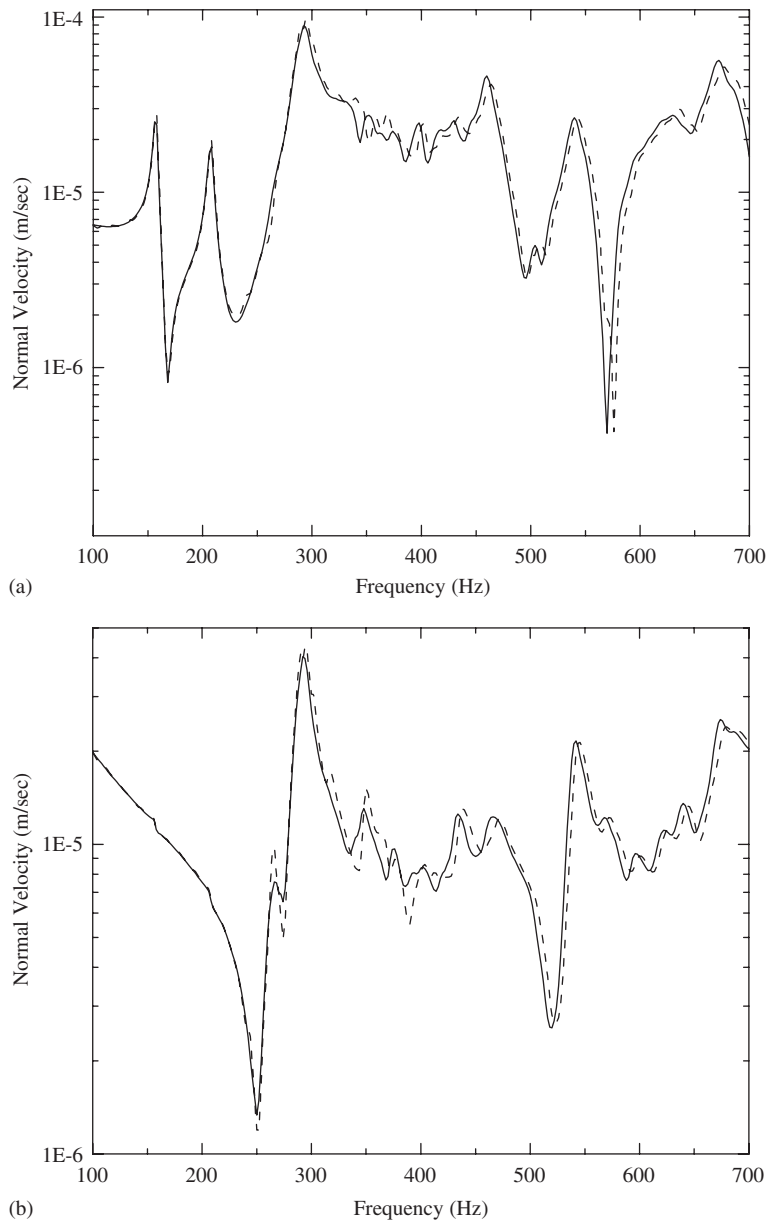|	Upper frame	Lower frame
Moment of inertia (m^4)	2.243e−7	5.745e−6
Area (m^2)	4.650e−4	1.129e−3

Fig. 9. Velocity at points 1 (a) and 2 (b) on the frame of the box structure when external excitation is applied in the *x*-directional excitation (see Fig. 4). ——— Hybrid FEA, - - - - conventional FEA.

force oriented along the *x* direction is applied at one of the lower corners of the box structure (Fig. 4). The locations on the stiff members where vibration results are compared from the FEA and the hybrid computations are identified in Fig. 4. The plates for which bending energy results are presented are also identified in Fig. 4. The velocities computed at nodes 1 and 2 by the FEA the hybrid FEA are compared in Fig. 9. The results demonstrate that the vibration of the stiff members is captured correctly by the hybrid method and that the interaction between stiff and flexible members is accounted properly by the addition of the damping elements. In order to demonstrate the importance of representing properly the flexible members when computing the behavior of the stiff members the damping elements which represent the presence of the flexible members are removed from the FEA model of the stiff members, and the vibration simulation are

repeated. Results for points 3 and 4 are presented in Fig. 10. The velocities are overestimated in the peaks and underestimated in the valleys when the damping elements are removed. The difference in the results can be explained by the mechanism of energy dissipation. If the power dissipation from the flexible members is not accounted properly in the model, then the response of the stiff members is not computed correctly. Thus, it is important to account properly for the effect of the flexible members on the structural vibration of the stiff members.

The input power in the system is presented in Fig. 11(a). The hybrid FEA evaluates the same input power with the dense FEA model. This agreement demonstrates that the hybrid FEA represents correctly the driving
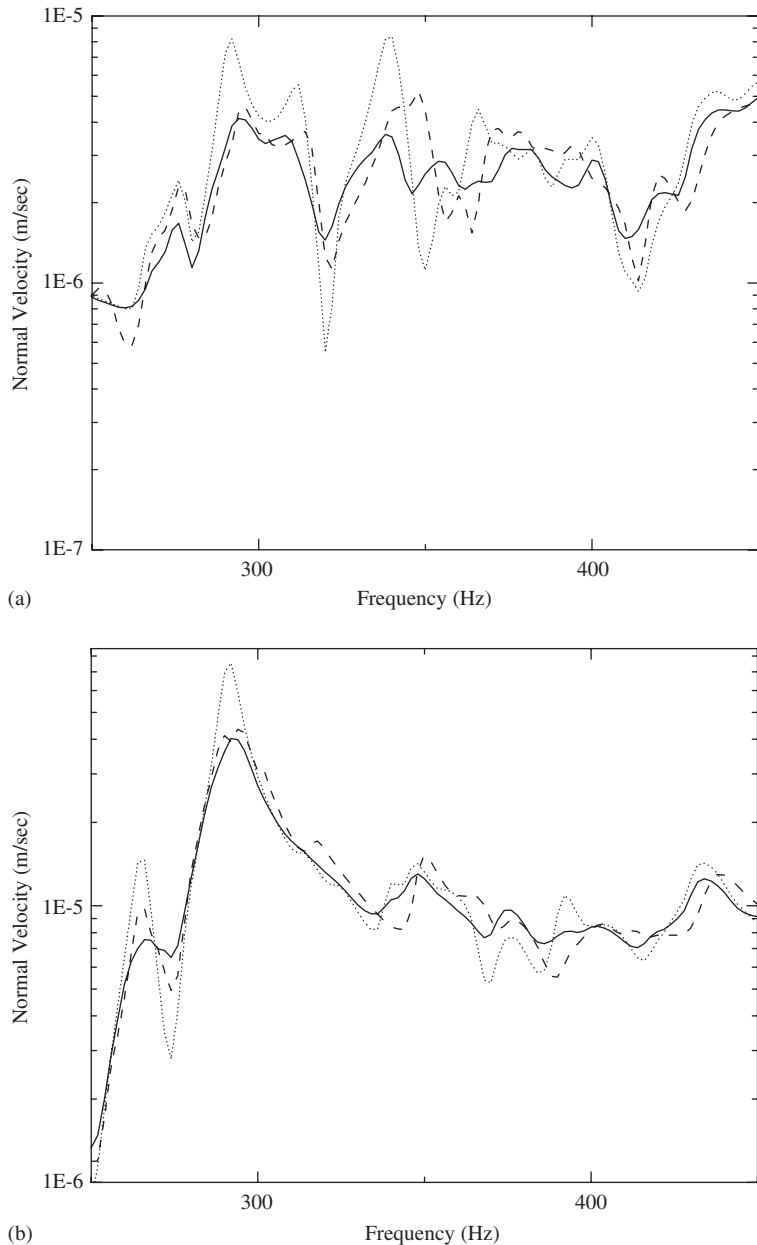
Fig. 10. Vibration at nodes 3 (a) and 4 (b) on the frame of the box structure when external excitation is applied in the x-direction. ——— Hybrid FEA, - - - - conventional FEA, · · · · · hybrid FEA without damper.
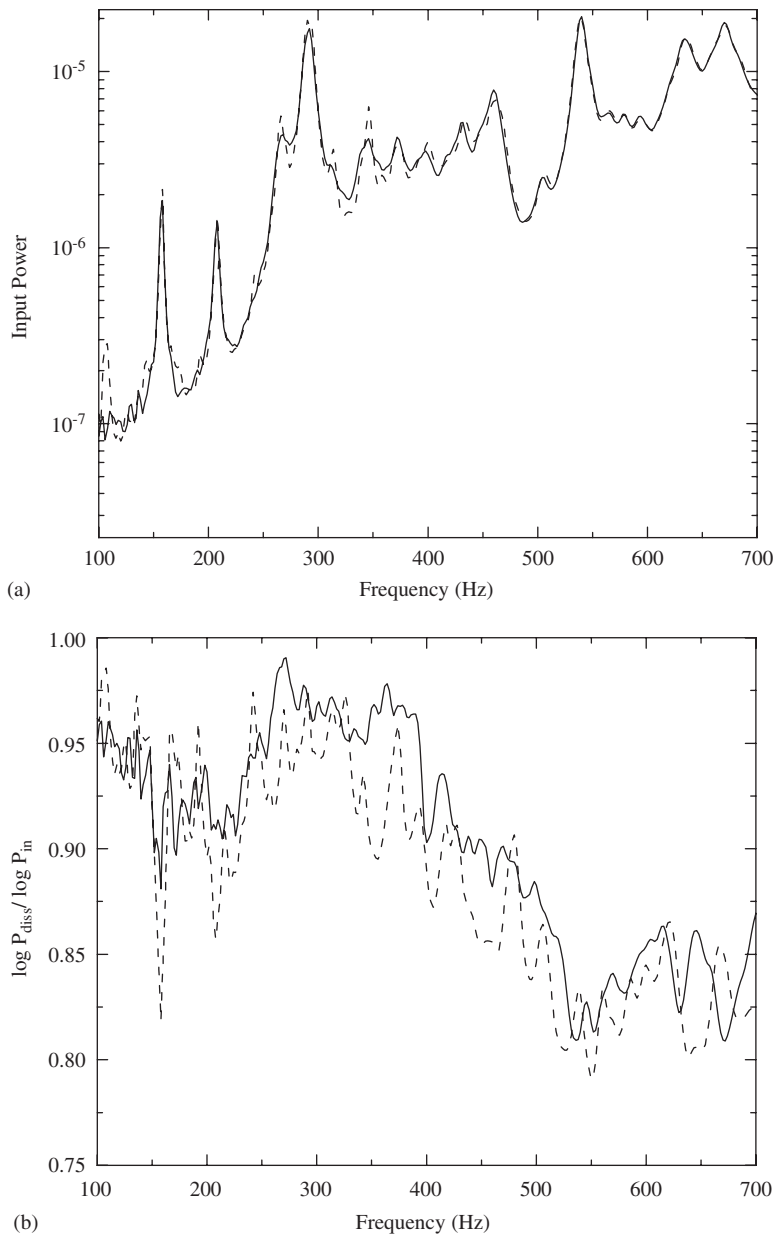
Fig. 11. (a) Input power and (b) ratio of dissipated power in the flexible members with respect to the input power when the external excitation is applied in the *x*-direction in the box structure (see Fig. 4). ———— Hybrid FEA, - - - - conventional FEA.

point admittance of the total structure in the frequency range of analysis. The ratio of the power dissipated in the flexible members with respect to the input power into the system is depicted in Fig. 11(b). Good agreement between the dense FEA results and the hybrid results is observed for the power flow into the flexible members and as expected all ratios are smaller than one. This is an indication that the power transfer mechanism to the flexible members is captured correctly by the hybrid FEA.

The total energy in the flexible members of the box structure is presented in Fig. 12(a). The corresponding energy in plate A (Fig. 4) is also presented in Fig. 12(b). In both sets of figures results are presented from the dense FEA and the hybrid FEA analyses. The results are presented both in 2 Hz increments and in
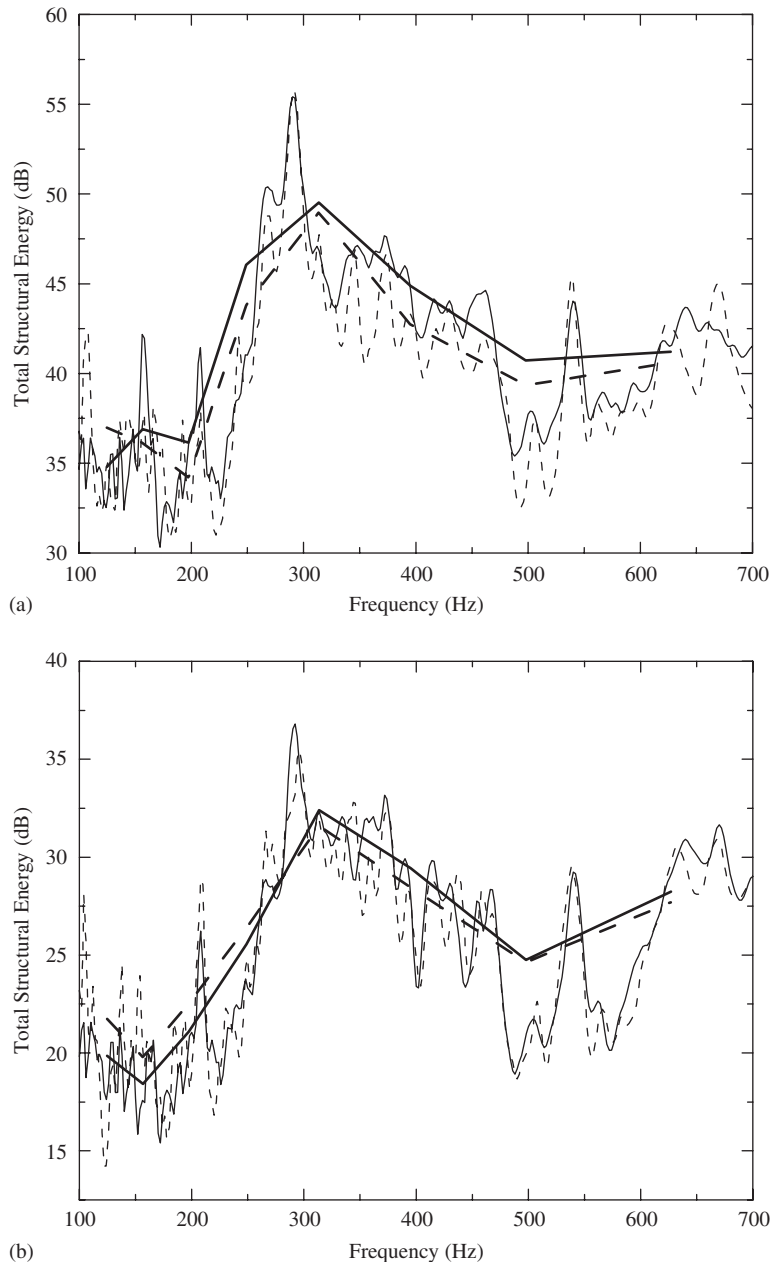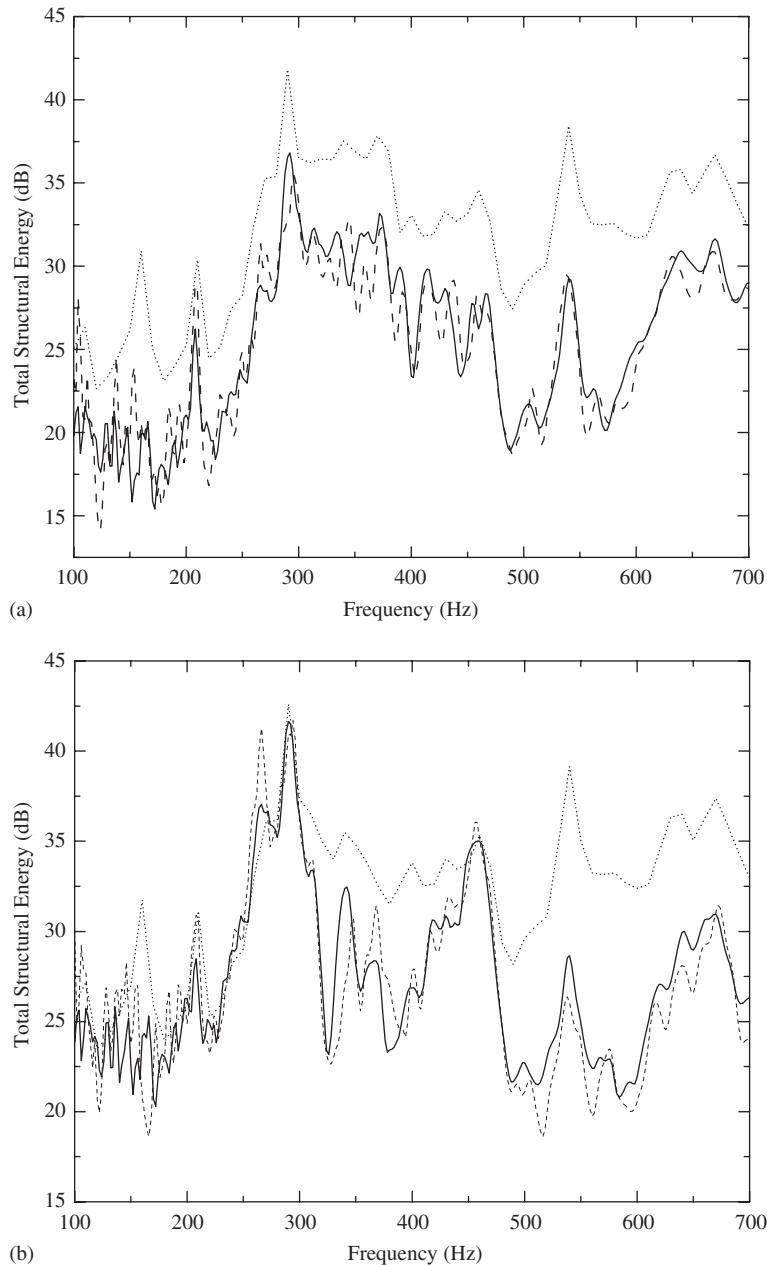
Fig. 12. Comparisons of energy in the flexible components of the box structure (a) sum of total flexible energy in all plates (b) flexible energy in plate A. External excitation is applied in *x*-direction in the box structure (see Fig. 4). ——— Hybrid FEA, - - - - conventional FEA, ——— hybrid FEA averaged in 1/3 octave band, - - - - conventional FEA averaged in 1/3 octave band.

Table 2
Comparison of degrees of freedom and CPU time for the complex model

	Hybrid FEA	Conventional FEA
Degrees of freedom	18,034	218,419
CPU time per frequency	18.4 s	239 s

Fig. 13. Comparisons of energy in the flexible components of the box structure (a) flexible energy in plate A (b) flexible energy in plate B. External excitation is applied in *x*-direction in the box structure (see Fig. 4). ——— Hybrid FEA, - - - - conventional FEA, · · · · · EFEA.

1/3 octave bands. The computational savings gained by the hybrid FEA are significant (Table 2) compared to the conventional dense FEA model. Good agreement is observed between the two methods. The good correlation indicates that the hybrid FEA captures correctly the resonant behavior of the short members, the coupling between the long and short members, the driving point admittance demonstrated by the system, and the power flow between stiff and flexible members. In order to demonstrate the importance of the new hybrid FEA formulation in computing mid-frequency vibrations, an EFEA analysis for the box structure is also performed. The input power evaluated by the dense FEA model is utilized as
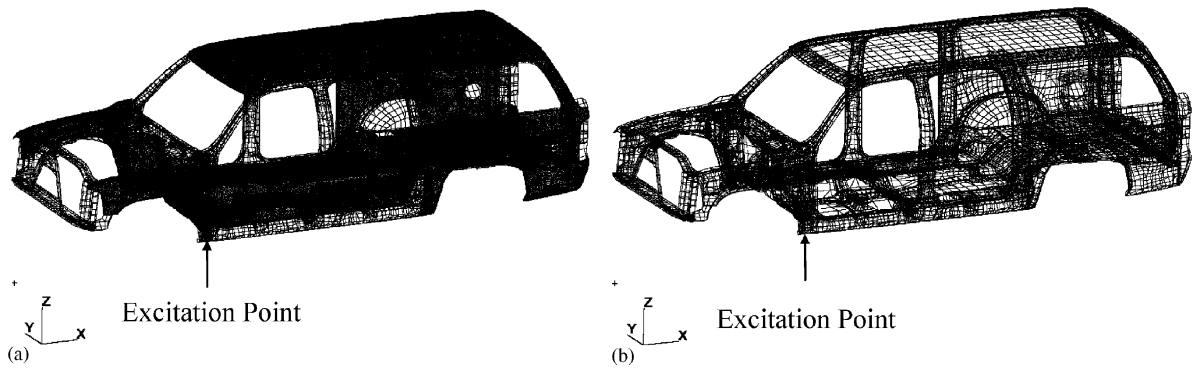
Fig. 14. Vehicle model for BIW (a) the conventional FEA: 714,172 dof (b) the hybrid FEA: 144,577 dof.

excitation for the EFEA computations since the EFEA does not have a mechanism for assessing accurately the driving point admittance of the overall system as a typical high-frequency method. The amount of energy in plates A and B is presented in Fig. 13. The hybrid FEA and the dense FEA results are also presented for reference. The EFEA results appear to follow somewhat the fluctuations in the values of the flexible energy, but this is the result of defining correctly the input power into the system from the dense FEA results. Otherwise, the EFEA could have not evaluated correctly the driving point admittance. The EFEA results diverge in comparison from the dense FEA solution and the hybrid FEA results since they cannot capture correctly the flow of power through the system due to the presence of the stiff members.

4.2.3. Analysis of an automotive body-in-white

An automotive body-in-white (BIW) is analyzed by the hybrid FEA and the results are compared to a dense FEA solution for validation. The FEA model of the vehicle is depicted in Fig. 14(a). The bending behavior of the four panels presented in Fig. 15 constitutes the flexible members of the model. The hybrid model is presented in Fig. 14(b). Detail information about the number of nodes and elements of the flexible members in the two models is summarized in Fig. 15. As in all previous validation cases, the effect of the flexible members on the stiff members, and the mechanism of power flow between stiff and flexible members is captured through the introduction of appropriate damping elements at the joint locations between stiff and flexible members. The appropriate damping coefficients are calculated for each one of the four major panels based on the dimensions, material, and physical properties of the flexible members. A concentrated force is applied at the lower front left end of the vehicle in both the FEA and the hybrid FEA models (Fig. 14). In the hybrid FEA the structural vibration of the stiff members is computed first. Based on the vibration at the joints between stiff and flexible members, the values of the damping elements the power flow from the stiff to the flexible members is determined according to Eq. (19). Then, the flexible members are analyzed using the EFEA and the amount of flexible energy in the flexible members is determined.

Velocities computed by the FEA and the hybrid FEA models at four characteristic locations at the edges of the four flexible panels (floor, roof, quarter panels, and dash) are in Figs. 16–19. The conventional and the hybrid FEA results present the same general trends and are in good agreement over the entire frequency range. The correlation between the two sets of results is similar to or better than typical observed between numerical results and test data for the structural vibration of vehicle structures [41,42]. The total bending energy for each one of the four flexible panels is computed by both methods and presented in Figs. 20 and 21. The vibration at every node of the dense finite element model is computed at every 2 Hz and the results for the corresponding energy are space averaged over an entire panel for each frequency of analysis. Good correlation is observed for both the results at individual frequencies and for the frequency averaged results at 1/3 octave bands. The computational savings gained by the hybrid FEA are significant (Table 3) compared to the conventional dense
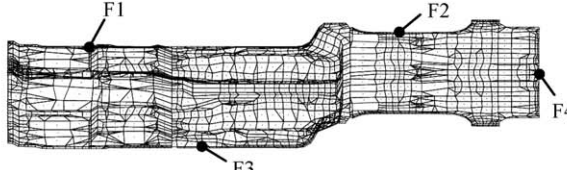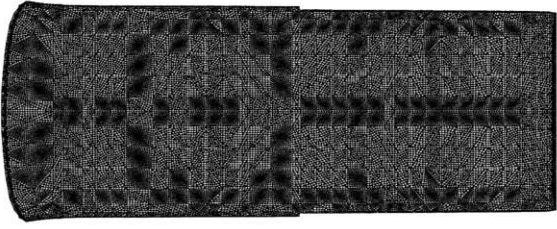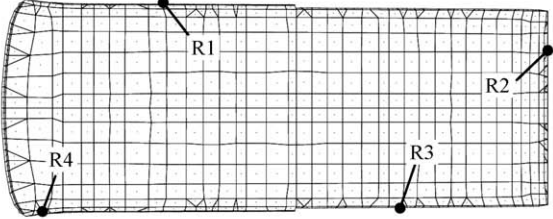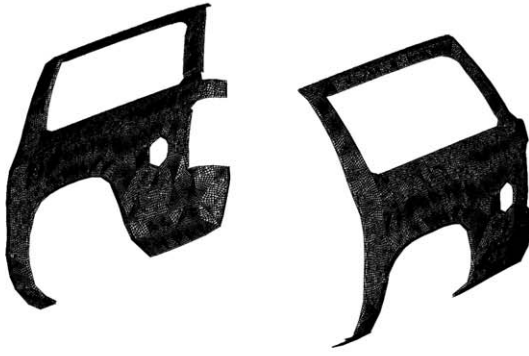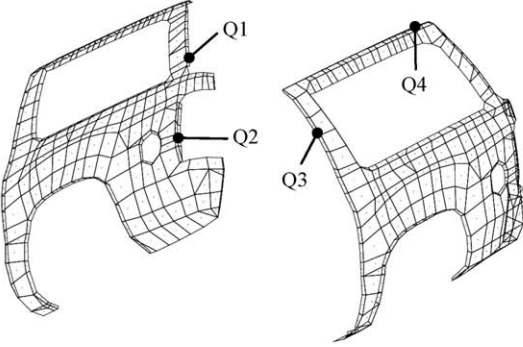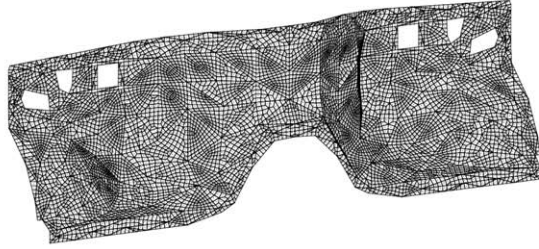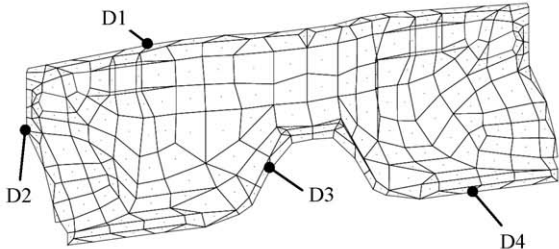
Conventional FEA model	Hybrid FEA model
42,612 nodes, 47,128 elements	2,032 nodes, 2,066 elements
29,871 nodes, 31,996 elements	733 nodes, 680 elements
26,328 nodes, 26,206 elements	716 nodes, 580 elements
7,945 nodes, 8,050 elements	295 nodes, 280 elements

Fig. 15. The individual panels which comprise the flexible members in the hybrid FEA are (starting from the top of the figure): floor panel, roof panel, quarter panel, and dash panel from the top.

FEA model. The dof in the hybrid FEA model are only 1/5 of the dof in the conventional FEA model, and the CPU time required by the hybrid method is 1/10 of the time required by the conventional FEA. In addition, significant memory savings are realized in terms of required memory and also disk space for storage of scratch files.
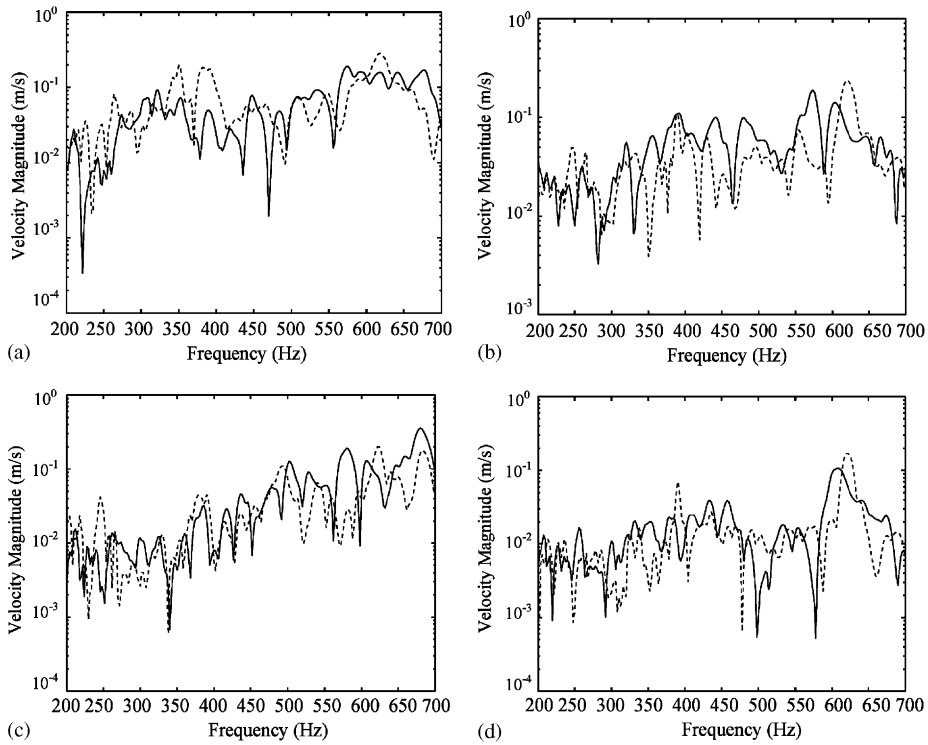
Fig. 16. Velocities at nodes placed at the edges around the floor panel of the vehicle model (see Fig. 15): (a) node F1, (b) node F2, (c) node F3, (d) node F4. ——— Hybrid FEA, - - - - conventional FEA.
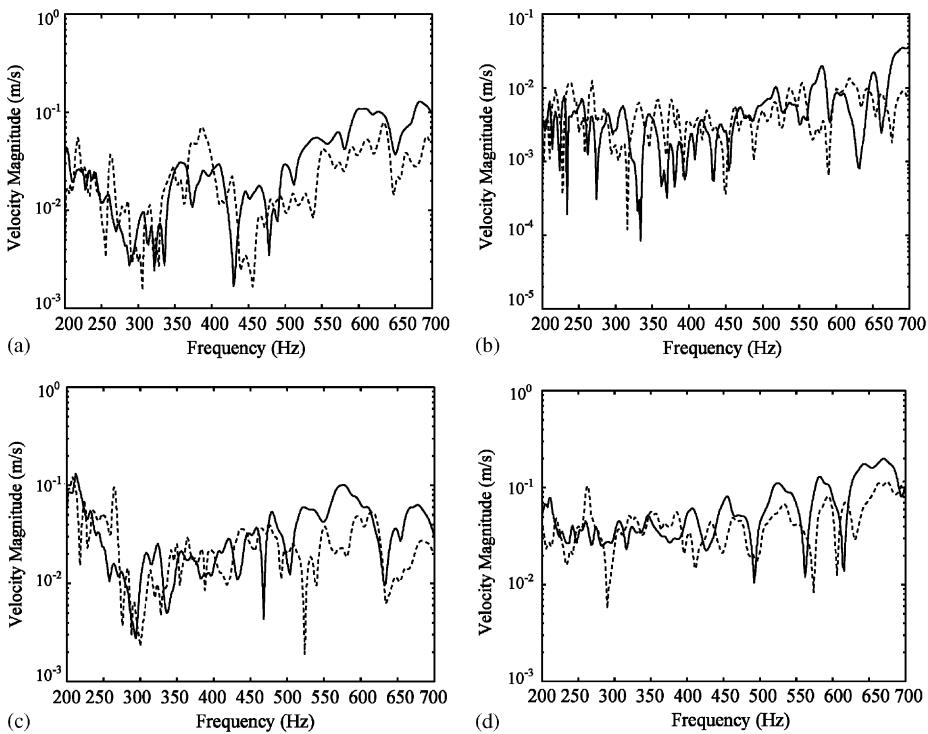

Fig. 17. Velocities at nodes placed at the edges around the roof panel of the vehicle model (see Fig. 15): (a) node R1, (b) node R2, (c) node R3, (d) node R4. ——— Hybrid FEA, - - - - conventional FEA.
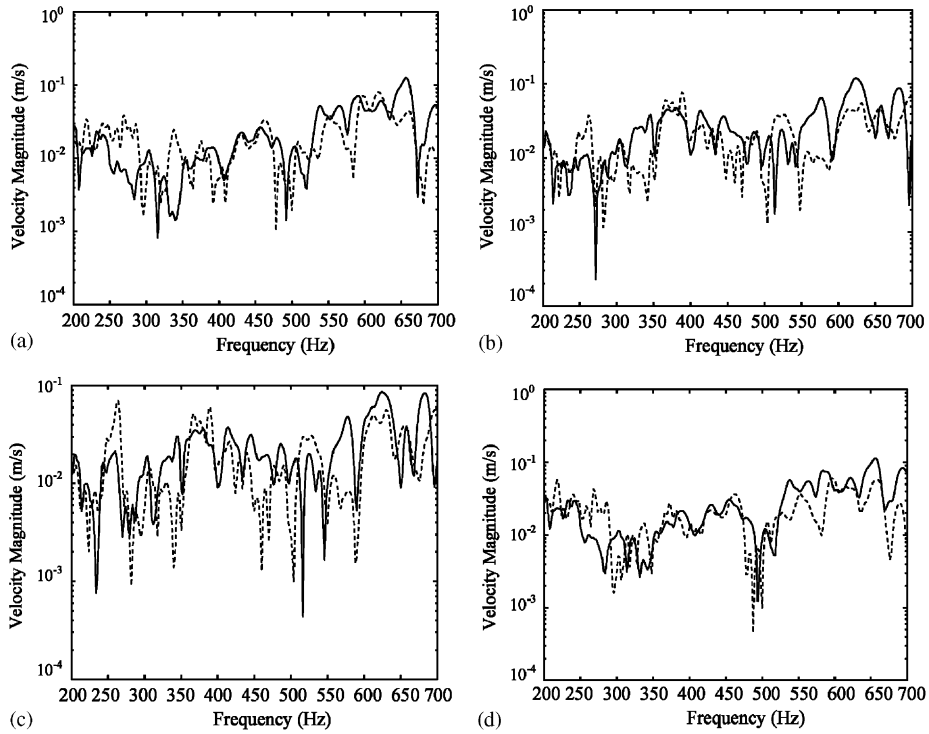
Fig. 18. Velocities at nodes placed at the edges around the quarter panel of the vehicle model (see Fig. 15): (a) node Q1, (b) node Q2, (c) node Q3, (d) node Q4. ——— Hybrid FEA, - - - - conventional FEA.
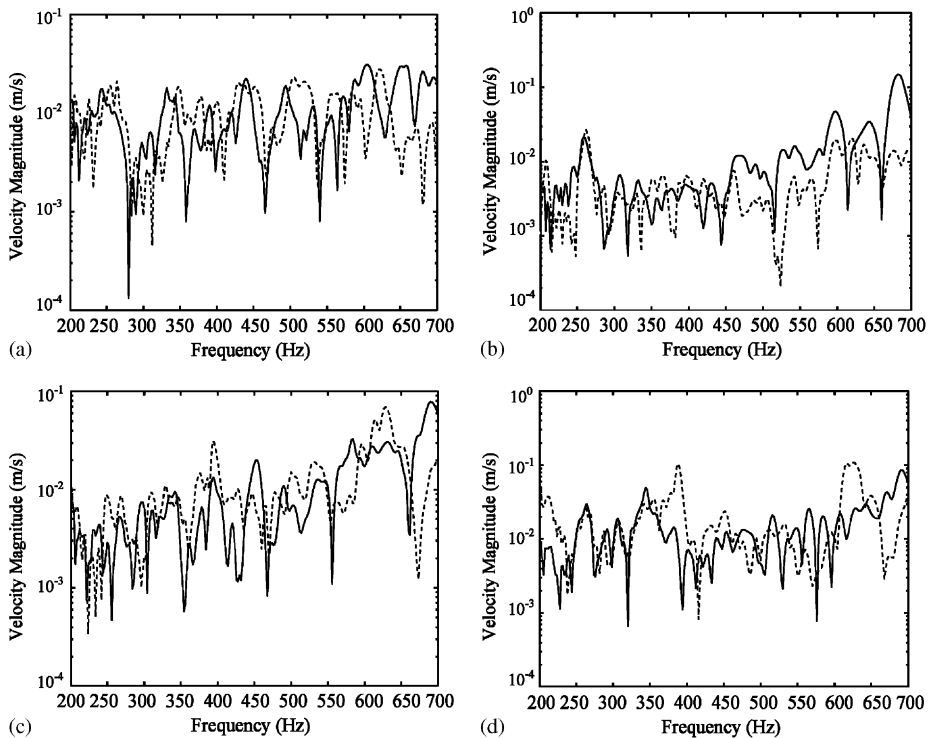

Fig. 19. Velocities at nodes placed at the edges around the dash panel of the vehicle model (see Fig. 15): (a) node D1, (b) node D2, (c) node D3, (d) node D4. ——— Hybrid FEA, - - - - conventional FEA.
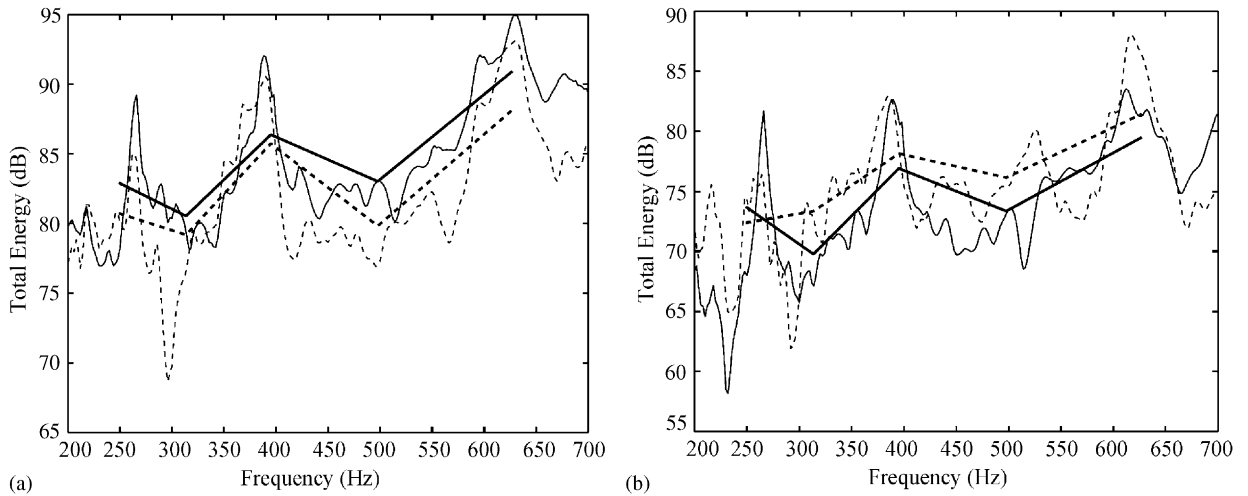
Fig. 20. Total bending energy (a) floor panel (b) roof panel. ——— Hybrid FEA, - - - - conventional FEA, ——— hybrid FEA averaged in 1/3 octave band, - - - - conventional FEA averaged in 1/3 octave band.
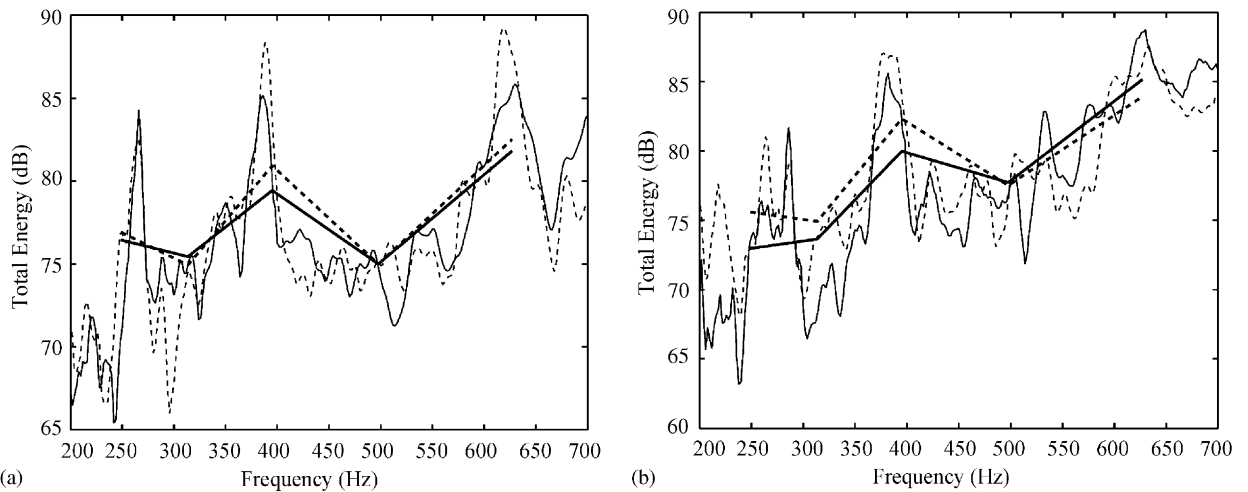

Fig. 21. Total bending energy (a) quarter panel (b) dash panel. ——— Hybrid FEA, - - - - conventional FEA, ——— hybrid FEA averaged in 1/3 octave band, - - - - conventional FEA averaged in 1/3 octave band.

Table 3
Comparison of dof, CPU time, amounts of memory and disk space for the vehicle model

	Hybrid FEA	Conventional FEA
Degrees of freedom	144,577	714,172
CPU time per frequency	85.25 s	952.9 s
Memory required	8,703,177 words	42,598,396 words
Disk space for scratch files	1,195,672 MB	6,547,125 MB

5. Conclusions

Hybrid FEA developments are presented in this paper for performing vibration analysis for systems of plates spot-welded to beam members. The flexible members are modeled by the EFEA and the stiff members

are modeled with conventional FEA. The bending behavior of the plates comprises the flexible members while the in-plane behavior of the plates and the beam members which provide the main structural integrity of the structural system comprise the stiff members. The external excitation is considered to be applied on the stiff members. The effect of the flexible members on the behavior of the stiff members is modeled by adding damping elements in the FEA model of the stiff members. The appropriate values of the damping elements are computed by evaluating the driving point conductance at the joints where the flexible members are spot-welded to the stiff members. The derivation of the driving point conductance is based on combining the CMS method with analytical equations for rectangular plates. The amount of power absorbed by the damping elements identifies the excitation for the EFEA analysis of the flexible members. Hybrid FEA solutions are validated through comparison to very dense FEA models for three structures of increasing complexity, a single plate attached to a frame, a box structure comprised of several plates attached to a frame, and an automotive BIW model. Physical properties which are compared are the vibration at discrete locations of the stiff members, the amount of energy in each flexible member, and the total amount of input power into the system due to a concentrated force excitation. The correlation between the hybrid FEA and the dense FEA is consistently very good.

Acknowledgments

References

[1] K.J. Bathe, *Finite Element Procedures in Engineering Analysis*, Prentice-Hall, New Jersey, 1982.
[2] K.H. Huebner, E.A. Thornton, *The Finite Element Method for Engineers*, Wiley, New York, 1982.
[3] M.A. Gockel, *MSC/NASTRAN Handbook for Dynamic Analysis*, The MacNeal-Schwendler Corporation, CA, 1983.
[4] J. Woodhouse, An approach to the theoretical background of statistical energy analysis applied to structural vibration, *Journal of the Acoustical Society of America* 69 (1991) 1695–1709.
[5] R.H. Lyon, R.G. DeJong, *Theory and Application of Statistical Energy Analysis*, Butterworth–Heinemann, Boston, 1995.
[6] C.B. Burroughs, R.W. Fischer, F.R. Kern, An introduction to statistical energy analysis, *Journal of the Acoustical Society of America* 101 (1997) 1779–1789.
[7] C.J. Radcliffe, X.L. Huang, Putting statistics into the statistical energy analysis of automotive vehicles, *Journal of Vibration and Acoustics* 119 (1997) 629–634.
[8] R.S. Thomas, J. Pan, M.J. Moeller, Implementing and improving statistical energy analysis models using quality technology, *Noise Control Engineering Journal* 45 (1997) 25–34.
[9] D.J. Nefske, S.H. Sung, Power flow finite element analysis of dynamic systems: basic theory and applications to beams, *Journal of Vibration and Acoustics* 111 (1989) 94–106.
[10] O.M. Bouthier, Energetics of Vibrating Systems, PhD Thesis, Purdue University, 1992.
[11] O.M. Bouthier, R.J. Bernhard, Simple models of the energetics of transversely vibrating plates, *Journal of Sound and Vibration* 182 (1995) 149–164.
[12] J.E. Huff, R.J. Bernhard, Prediction of high frequency vibrations in coupled plates using energy finite element, *Proceedings of Inter-Noise*, Newport Beach, CA, 1995, pp. 1221–1226.
[13] O.M. Bouthier, R.J. Bernhard, Models of space averaged energetics of plates, *American Institute of Aeronautics and Astronautics Journal* 30 (1992) 138–146.
[14] N. Vlahopoulos, X. Zhao, T. Allen, An approach for evaluating power transfer coefficients for spot-welded joints in an energy finite element formulation, *Journal of Sound and Vibration* 220 (1999) 135–154.
[15] N. Vlahopoulos, L.O. Garza-Rios, C. Mollo, Numerical implementation, validation, and marine applications of an energy finite element formulation, *Journal of Ship Research* 43 (1999) 143–156.
[16] W. Zhang, A. Wang, N. Vlahopoulos, K. Wu, High-frequency vibration analysis of thin elastic plates under heavy fluid loading by an energy finite element formulation, *Journal of Sound and Vibration* 267 (2003) 21–46.
[17] W. Zhang, A. Wang, N. Vlahopoulos, An alternative energy finite element formulation based on incoherent orthogonal waves and its validation for marine structures, *Finite Elements in Analysis and Design* 38 (2002) 1095–1113.
[18] B.R. Mace, The statistical energy analysis of two continuous one-dimensional subsystem, *Journal of Sound and Vibration* 166 (1993) 429–461.
[19] J.K. Bennighof, M.F. Kaplan, M. Kim, Implementing automated multi-level substructuring in Nastran vibroacoustic analysis, *Proceedings of 2001 SAE Noise & Vibration Conference and Exposition*, Traverse City, MI, SAE Paper 2001-01-1405.

[20] M.P. Castanier, Y.C. Tan, C. Pierre, Characteristic constraint modes for component mode synthesis, *American Institute of Aeronautics and Astronautics* 39 (2001) 1182–1187.

[21] G. Zhang, M.P. Castanier, C. Pierre, Vibration and power flow analysis of a vehicle structure using characteristic constraint modes, *Proceedings of 2003 SAE Noise & Vibration Conference and Exposition*, Traverse City, MI, SAE Paper 2003-01-1602.

[22] C. Soize, A model and numerical method in the medium frequency range for vibroacoustic predictions using the theory of structural fuzzy, *Journal of the Acoustical Society of America* 94 (1993) 849–865.

[23] R. Ohayon, C. Soize, *Structural Acoustics and Vibration*, Academic Press, New York, 1998.

[24] C. Soize, Reduced models in the medium frequency range for general dissipative structural-dynamics systems, *European Journal of Mechanics—A/Solids* 17 (1998) 657–685.

[25] C. Soize, Reduced models in the medium-frequency range for general external structural-acoustic systems, *Journal of the Acoustical Society of America* 103 (1998) 3393–3406.

[26] C. Soize, Reduced models for structures in the medium-frequency range coupled with internal acoustic cavities, *Journal of the Acoustical Society of America* 106 (1999) 3362–3374.

[27] C. Soize, K. Bjaoui, Estimation of fuzzy structure parameters for continuous junctions, *Journal of the Acoustical Society of America* 107 (2000) 2011–2020.

[28] B.R. Mace, P.J. Shorter, Energy flow models from finite element analysis, *Journal of Sound and Vibration* 233 (2000) 369–389.

[29] R.M. Grice, R.J. Pinnington, A method for the vibration analysis of built-up structures, part I: introduction and analytical analysis of the plate-stiffened beam, *Journal of Sound and Vibration* 230 (1999) 825–849.

[30] R.M. Grice, R.J. Pinnington, A method for the vibration analysis of built-up structures, part II: analysis of the plate-stiffened beam using a combination of finite element analysis and analytical impedances, *Journal of Sound and Vibration* 230 (2000) 851–875.

[31] L. Lu, Dynamic substructuring by FEA/SEA, *Winter Annual Meeting of the American Society of Mechanical Engineers*, Dallas, TX, November 1990, pp. 9–12.

[32] R.S. Langley, P. Bremner, A hybrid method for the vibration analysis of complex structural-acoustic systems, *Journal of the Acoustical Society of America* 105 (1999) 1657–1671.

[33] N. Vlahopoulos, X. Zhao, Basic development of hybrid finite element method for mid-frequency structural vibrations, *American Institute of Aeronautics and Astronautics Journal* 37 (1999) 1495–1505.

[34] X. Zhao, N. Vlahopoulos, A hybrid finite element formulation for mid-frequency analysis of systems with excitation applied on short members, *Journal of Sound and Vibration* 273 (2000) 181–202.

[35] N. Vlahopoulos, X. Zhao, An investigation of power flow in the mid-frequency range for systems of co-linear beams based on a hybrid finite element formulation, *Journal of Sound and Vibration* 242 (2001) 445–473.

[36] X. Zhao, N. Vlahopoulos, A basic hybrid finite element formulation for mid-frequency analysis of beams connected at an arbitrary angle, *Journal of Sound and Vibration* 269 (2004) 135–164.

[37] W.C. Hurty, Dynamic Analysis of Structural Systems using component modes, *American Institute of Aeronautics and Astronautics Journal* 3 (1965) 678–685.

[38] R.R. Craig, M.C.C. Bampton, Coupling of substructures for dynamic analysis, *American Institute of Aeronautics and Astronautics Journal* 6 (1968) 1313–1319.

[39] M.S.C. Nastran, *2001 Quick Reference Guide*, The MacNeal-Schwendler Corporation, CA, 2001.

[40] L.L. Beranek, I.L. Ver, *Noise and Vibration Control Engineering*, Wiley, New York, 1992.

[41] S.H. Sung, D.J. Nefske, Assessment of a vehicle concept finite-element model for predicting structural vibration, *Proceedings of 2001 SAE Noise & Vibration Conference and Exposition*, Traverse City, MI, SAE Paper 2001-01-1402.

[42] A. Sol, F. VanHerpe, Numerical prediction of a whole car vibro-acoustic behavior at low frequencies, *Proceedings of 2001 SAE Noise & Vibration Conference and Exposition*, Traverse City, MI, SAE Paper 2001-01-1521.